# Effect of indium pre-flow on wavelength shift and crystal structure of deep green light emitting diodes

# Effect of indium pre-flow on wavelength shift and crystal structure of deep green light emitting diodes

**SHAMSUL AMIR ABDUL RAIS,**[1,2,3,*] **ZAINURIAH HASSAN,**[1] **AHMAD SHUHAIMI ABU BAKAR,**[4] **MOHD NAZRI ABD RAHMAN,**[4] **YUSNIZAM YUSUF,**[4] **MUHAMAD IKRAM MD TAIB,**[1] **ABDULLAH FADIL SULAIMAN,**[4] **HAYATUN NAJIHA HUSSIN,**[4] **MOHD FAIRUS AHMAD,**[2,3] **MOHD NATASHAH NORIZAN,**[2,3] **KEIJI NAGAI,**[5] **YUKA AKIMOTO,**[5] **AND DAI SHOJI**[5]

[1]*Institute of Nano Optoelectronics Research and Technology (INOR), Universiti Sains Malaysia, 11800, USM, Penang, Malaysia*
[2]*Faculty of Electronic Engineering Technology, Universiti Malaysia Perlis, Kampus Alam Pauh Putra, 02600 Arau, Perlis, Malaysia*
[3]*Centre of Excellence Geopolymer and Green Technology (CeGeoGTech), Universiti Malaysia Perlis, Perlis, Malaysia*
[4]*Universiti Malaya, 50603, Kuala Lumpur, Malaysia*
[5]*Laboratory for Chemistry and Life Science, Institute of Innovative Research, Tokyo Institute of Technology, R1-26, Nagatsuta 4259, Midori-ku, Yokohama 226-8503, Kanagawa, Japan*
*[*]shamsulamir@unimap.edu.my*

**Abstract:** To produce a deep green (530 nm–570 nm) LED, the suitable indium (In) composition in the $In_xGa_{1-x}N$/GaN multi-quantum well (MQW) structure is crucial because a lower indium composition will shift the wavelength of emission towards the ultraviolet region. In this paper, we clarify the effects of an indium-rich layer to suppress such blue shifting, especially after the annealing process. According to characterizations by the uses of XRD and TEM, narrowing of the MQW layer was observed by the indium capping, while without the capping, the annealing results in a slight narrowing of MQW on the nearest layer to the p-type layer. By adding an indium capping layer, the blue shift of the photoluminescence was also suppressed and a slight red shift to keep green emission was observed. Such photoluminescence properties were consistent with the tiny change of the MQW as seen in the XRD and TEM characterizations.

## 1. Introduction

One of the main targets in Light Emitting Diode(LED) research is to broaden the emission wavelength range [1]. $In_xGa_{1-x}N$ has the direct bandgap between 0.6eV to 3.4 eV which is the bandgap between InN and GaN [2]. This spans between the infrared region and the ultraviolet region in terms of light emissions. Due to this property, the indium became the main element alloyed in the multi-quantum well (MQW) to achieve blue, green, or other longer wavelengths in LED fabrication. We are attracted to fabricate LED in a deep green region is around 530-570nm region, which has some advantages in an application such as good light efficacy [3], satisfied luminous sensation for eyes [4], great color rendering index [5] and promising candidate in light fidelity(Li-Fi) light source [6].

To fabricate LEDs that produce light with a wavelength in the deep green region, we need high indium content within the MQW [7]. However, since indium has a very low melting point compared to the housing GaN crystal, a problem occurs when the full LED device is further annealed as indium escapes from the MQW as it is very thin [8,9]. The LED uses magnesium as

its p-type dopant which needed to be annealed to remove the hydrogen complex which decreased the holes carrier performance [10–12]. The out diffuse of indium from MQW causes the LED light emissions to shift from green to blue region [13]. The need to maintain high indium content in the MQW after the complete fabrication process is crucial.

A lot of research towards green LED has been done in the past [14–17] which succeeded to achieve the green region of light emissions, but it did not reach the deep green region or encounter other problems. One of the techniques is to grow the MQW layer at a lower temperature around 550-600°C to incorporate more indium. Although succeeded in emitting deep green wavelength, they lack in the narrow spectrum as required as LED standard, and sometimes demonstrate double peaks. These phenomena are a result of crystal defect due to too much indium alloyed at these low temperature, that leads to deep band recombination [18,19]. These problems degraded some roles of MQW such as increasing indium content within the LED and increase its brightness [20,21].

From these explanations, it is understood that it is crucial to fabricate not just LED with high indium content in the MQW, but also has good crystal quality to have a narrow, single-peak spectrum. The amount of indium that can be incorporated during the MQW growth phase at a temperature that produces low defect crystals might have its limits, so finding a way of preventing the indium out diffuse, or even a mechanism that enhanced the indium content during the p-type activation via annealing process is inevitable. Previous research has reported indium pre-flow technique in their blue LED fabrication [22] even though the indium diffused out from MQW was almost unnoticed. A similar approach on the green LED [23,24] had been done, even though they didn't emphasize much on crystal quality which determines the full-width half maximum (FWHM) of the outcome light spectrum.

In this paper, we approached the indium pre-flow technique to fabricate deep green LEDs. The idea was to create a high indium concentration region beneath the MQW which will become the top part of the *n*-type crystal structure so that the indium in the MQW cannot diffuse downwards when the device is annealed. We did not apply indium on top of the MQW as capping since the structure already has the AlGaN cap which also acts as the electron blocking layer (EBL). We used C-plane GaN for the substrate. We had fabricated various samples with different III-V ratios and compositions of the GaN cap, so there can be a comparison between those optimizations.

## 2.    Experimental procedures

As mentioned in the introduction part, we prepared five samples, namely samples A, B, C, D, and E. Sample A has the basic recipe without indium pre-flow. Sample B, C, D, and E all have the indium pre-flow. The samples C and E had more nitrogen in the III-V ratio in the MQW and the samples D and E do not have aluminum capping on the GaN. These samples can be simplified as the following table (Table 1).

**Table 1. The table of samples and alteration undergone**

| Sample | Indium Pre-flow | Nitrogen Increased | Aluminum in GaN Cap | Wavelength shift |
|--------|-----------------|--------------------|---------------------|------------------|
| A | No | No | Yes | Blue (−45 nm) |
| B | Yes | No | Yes | Green (+3 nm) |
| C | Yes | Yes | Yes | Blue (−27 nm) |
| D | Yes | No | No | No Significant Change (−1 nm) |
| E | Yes | Yes | No | No Significant Change (0 nm) |

Figure 1 shows the structural diagram of the full LED devices. The full LED epitaxy growth was carried out in Metal-Organic Vapor Chemical Deposition (MOCVD). The temperature of the MQW growth was 700 °C and the pressure was 0.5 Torr. For the *n*-type layer growth, the
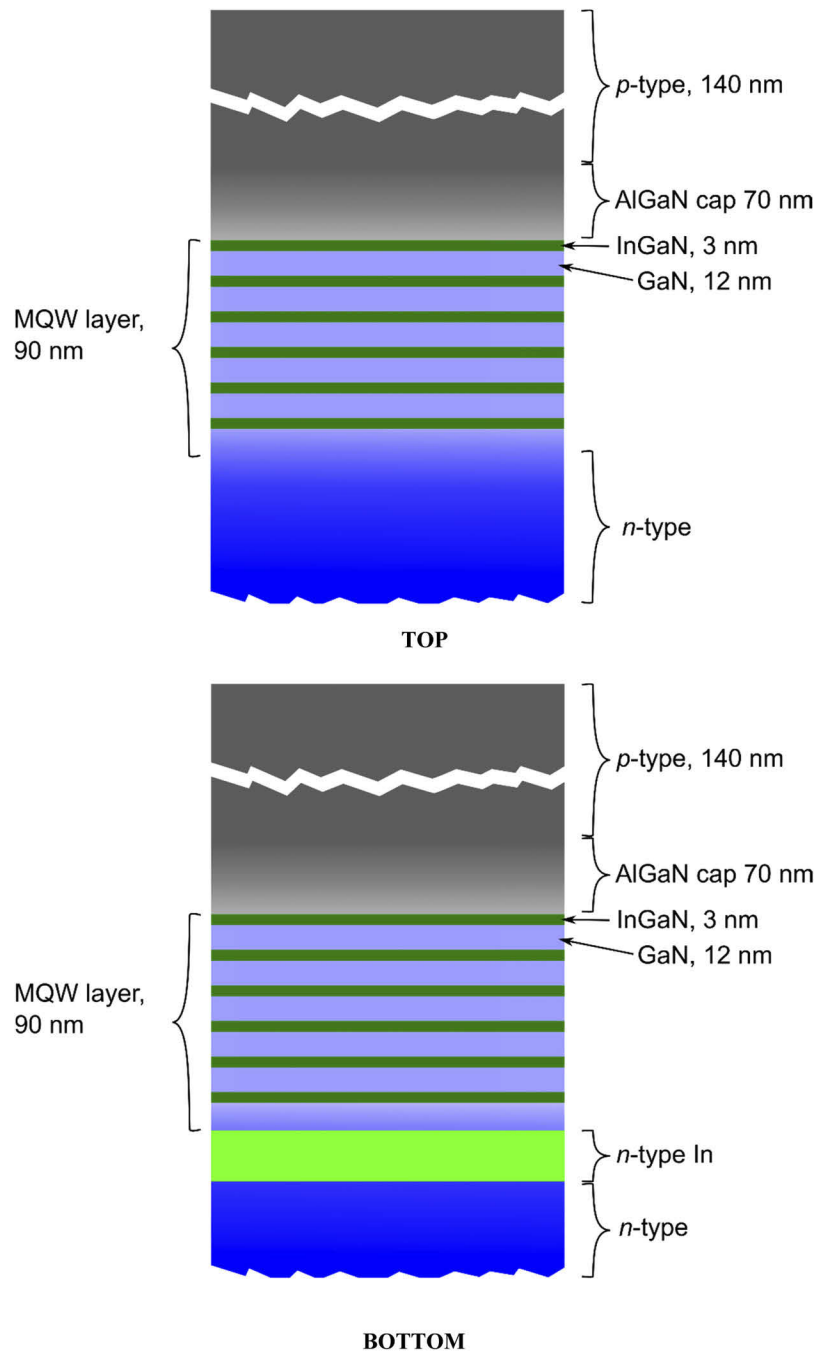
**TOP**



**BOTTOM**

**Fig. 1.** The basic structure of an LED grown. The top shows the structure of the LED without the indium pre-flow, and the bottom shows the structure with indium pre-flow.

temperature was set to be 1000 °C, and the temperature of EBL and P-type layer growth was 800°C. The pressure for these layers' growth was also 0.5 Torr. C -plane GaN (0 0 1) was used as the substrate. The base of the device which was a 5000nm $n$-type layer was grown from $NH_3$, trimethylgallium (TMG), and disilane ($Si_2H_6$) as sources for nitrogen, gallium, and silicon as dopant. For samples with an additional indium enriched crystal layer, trimethylindium (TMI) flowed in the chamber in the final stage of the $n$-type growth as the source of indium. All the samples except for sample A undergo this step, which we called *pre-flow*. During this step, parameters such as temperature and pressure remain the same as the $n$-type growth phase, but the flow of TMI was maximized to 400 standard cubic centimeters per minute (SCCM). The MQW consists of six pairs of GaN/ $In_xGa_{1-x}N$ layers which were grown from $NH_3$, Triethylgallium (TEG), and TMI as sources or nitrogen gallium and indium, respectively. The ratio of gallium/indium was set as 1:6 for the $In_xGa_{1-x}N$ layers and they were grown alternately to form six pairs of 12nm/3nm GaN/ $In_xGa_{1-x}N$ sets of MQW. The total thickness of the MQW was set to be 90nm. On top of the MQW, a layer of 70nm AlGaN cap layer was grown from $NH_3$, TMG, and trimethylaluminum (TMA) as the sources for nitrogen, gallium, and aluminum. For samples D and E, only TMG and $NH_3$ flowed during this step. Finally, the topmost layer of the LED devices was made up of a 140nm layer of $p$-type which was grown from TMG, $NH_3$, and bis(cyclopentadienyl)magnesium(II) ($Cp_2Mg$) as the source of gallium, nitrogen, and magnesium as a $p$-type dopant. The photoluminescence test was done right after the epitaxy growth was finished and after the annealing process for $p$-type activation was done. The annealing was done in a furnace with a temperature of 650 °C for 15 minutes. The samples were cut into two pieces, one was kept without annealing and the other was annealed for comparison reason. Sample A after the annealing process, sample B before the annealing process, and sample B after annealing were examined using transmission electron microscopy (TEM). The samples were prepared using the focus ion beam (FIB) milling technique before observed under TEM (JEM-2100F, JEOL), after the protection of carbon coating (JIB-4500, JEOL).

## 3. Results and discussion

### 3.1. Photoluminescence spectrum

Figure 2 shows the photoluminescence (PL) spectrum of samples A, B, and C. The incident laser for this measurement was a 430 nm UV laser. Sample A gives a peak value of 568 nm before the annealing. However, the photoluminescence spectrum after the annealing process changed to 523 nm, a big shift towards the blue/UV range. This phenomenon can be viewed as the result of indium loss from the MQW [25,26]. This problem does not occur or has a significant effect on blue LED or other LED with lower indium content, but as the indium incorporated into the MQW increase, the probability of the indium dissipation increased since indium has a very low melting point, 156.60 °C. It also makes it hard to fabricate a green LED with a specifically targeted wavelength range since the shift is too big. This result triggers us to apply the indium pre-flow technique before the growth of the MQW layer, which would turn into the structure, as shown in Fig. 1. The outcome gives a convincing result. The PL spectrum of sample B gives 548 nm before the annealing process and 551 nm after the annealing process. It shows that the indium pre-flow would not just prevent the indium loss from the MQW, inversely it shifted the wavelength towards the green/red region of wavelength. This phenomenon can be interpreted as a result of indium diffused from the much higher concentration crystallized indium layer beneath the MQW into the MQW. The sample C would contain higher nitride in the MQW since higher V content in III-V ratio would give better crystal quality [27], in case we need to put more indium in the MQW and at the same time trying to reduce the dislocation. The PL spectrum shows that increased nitride while growing the MQW decreased the wavelength to 500 nm even before annealing, possibly due to a lower indium nucleation rate [28], and further shifted to the blue region of 473 nm after annealing. Nevertheless, the shift was greatly reduced from 45 nm for

sample A to 27 nm for sample C. The pre-flow indium does have its effect. Sample D has a peak wavelength of 508 nm before annealing and 507 nm after annealing, and sample E has a peak wavelength of 530 nm before annealing and remains 530 nm after annealing. Both these samples also proved that the indium pre-flow does help prevent or at least reduced blue-shift for the green LED. The absence of aluminum in these samples cap might have effects on the LED electrical characteristic since the cap also acts as the electron blocking layer, but we will not be discussing that in this paper. Sample C shows a larger peak shift than sample E before and after annealing. These phenomena can be hypothesized as the indium diffusion rate from the MQW to the top and the bottom adjacent layers is the same. Since the thickness of the top layers is far smaller compared to the bottom layers, then the space that the diffused indium can occupied is much lesser at the top than the bottom. Thus, the amount of indium that can diffused to the bottom layers in sample C is more than the amount of indium that can diffused to the top layer in sample E. That would be why the peak shift is greater in sample C compared to sample E.
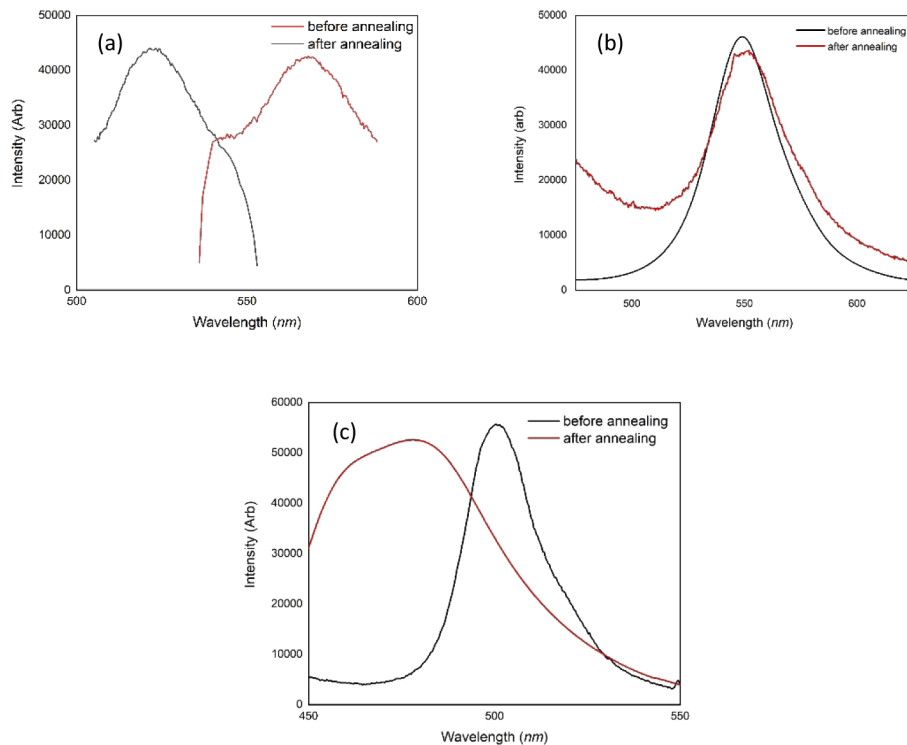


**Fig. 2.** The photoluminescence (PL) spectrum of (a) sample A, (b) sample B, and (c) sample C. The black line gives the spectrum of the samples before the annealing process, and the red line gives the spectrum after the annealing process.

### 3.2. XRD measurement results

Figure 3 exhibits the omega2theta scan of sample B before and after the annealing. The successions of peak and slopes represent GaN/ $In_xGa_{1-x}N$ MQW film sets which are six respectively. This sequence proved the existence of comparatively thin sets of layers in the MQW that are consistent with the desired structure. The result confirms there is no structural change from the annealing process although it does alter the indium content of the MQWs. All other omega2theta scans of other samples demonstrate the same pattern. GaN/ $In_xGa_{1-x}N$ layer thickness attained was 17.1 nm and 3.3 nm respectively from the simulation plot.
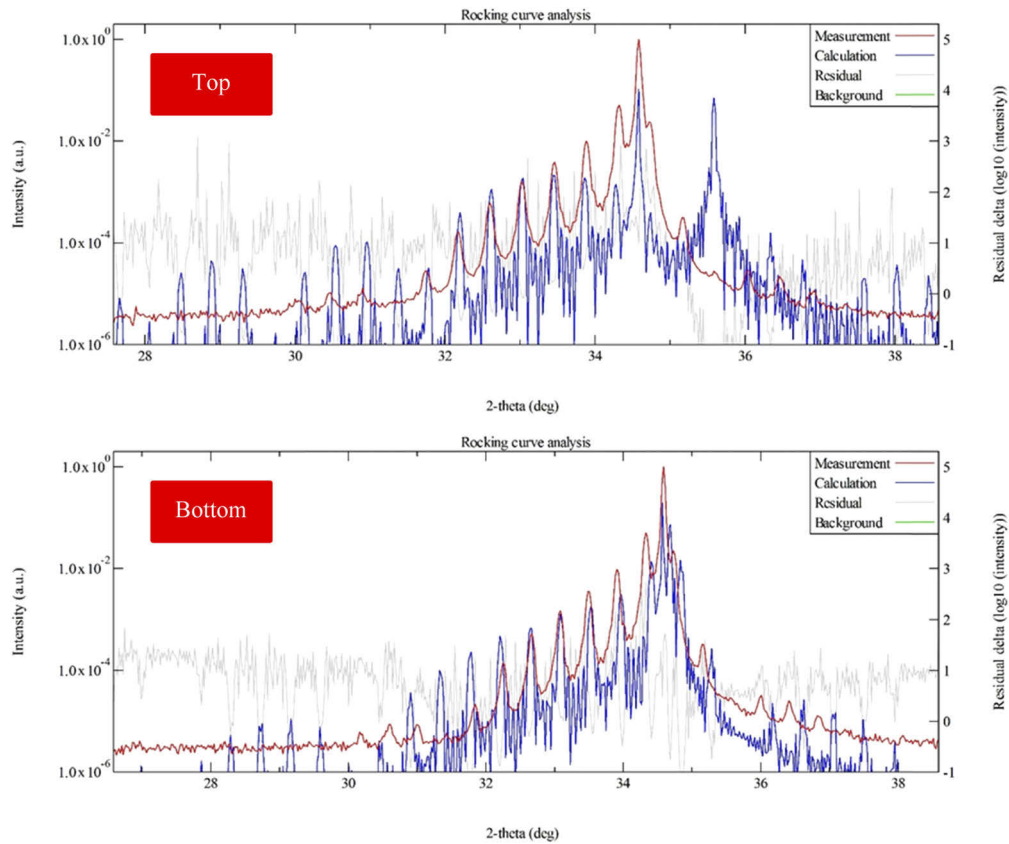
**Fig. 3.** The omega2theta result for sample B before annealing (top) and after annealing (bottom).

We also obtained the concentration of indium in the $In_xGa_{1-x}N$ layer from omega2theta calculation as in Table 2.

**Table 2. The concentration of indium in the $In_xGa_{1-x}N$ layer from 2theta calculation**

| Sample | Concentration Before Annealing % | Concentration After Annealing % | The difference,x % |
|--------|----------------------------------|----------------------------------|--------------------|
| A | - | 22 | - |
| B | 23 | 24 | +1 |
| C | 18 | 14 | −4 |
| D | 22 | 22 | 0 |
| E | 21 | 22 | +1 |

We can use the PL wavelength shift data to calculate the indium loss from the MWQ using Vegard's Law formula equation from Ref. [29] which is as follows:

$$E_g^{InGaN} = x \times E_g^{InN} + (1-x) \times E_g^{GaN} -- b \times x(1-x) \tag{1}$$

Where $E_g^{InGaN}$ is calculated from the wavelength, $E_g^{InN} = 0.77$ eV, $E_g^{GaN} = 3.39$ eV, b = 2.96 eV. All of these parameters are also obtained from Ref. [29] From the equation above and the values of the constants and the wavelengths of each of the samples, we can deduce that the value of incorporated indium in the $In_{(x)}Ga_{(1-x)}N$ are as in Table 3.

**Table 3.** The concentration of indium in the In$_x$Ga$_{1-x}$N
layer from Vagard's Law calculation

| Sample | Wavelength shift, nm | Difference, x, % |
|:------:|:--------------------:|:----------------:|
| A | −45 | −4.6 |
| B | +3 | +0.02 |
| C | −27 | −2.4 |
| D | −1 | ~0 |
| E | ~0 | ~0 |

The $x$ value from the XRD simulation and Vagard's Law formula shows a slight difference, but not in great order. The other explanation is that the omega2theta calculation of indium is for the entire structure, while the Vagard's Law calculation value is specified for the MQW indium loss.

The x-ray rocking curve characteristic can be observed in Fig. 4. We can obtain the crystal quality of the sample in terms of dislocation. Both curves for sample B before and after the annealling gives peaks at 17.25°, which is the peak for (0,0,2) GaN [30,31]. These curves also have the same FWHM 0.006741°, which is much better than the results of crystal quality of the same green MQW in [7]. These values indicate that the loss of indium gives nearly no effect on the crystal quality, and other samples behave the same. To further determine the quality of this crystal, we can calculate the dislocation, $\rho$, of the crystals by using Eq. (2) from Ref. [32]

$$\rho = \beta^2 \div ((4.35)b^2) \tag{2}$$

where $\beta$ is the FHWM value in radian, and b is the magnitude of the $b$ vector. Vector $b$ satisfies the equation $g.b = 0$, where g is the diffraction vector of XRC. The value of $b$ is $5.19 \times 10^{-8}$. From the calculation, we obtain the dislocation of the crystal was $\rho = 1.17 \times 10^5$ cm$^{-2}$. This value proves that the samples have a very low defect compared to [21] and [32], even with the
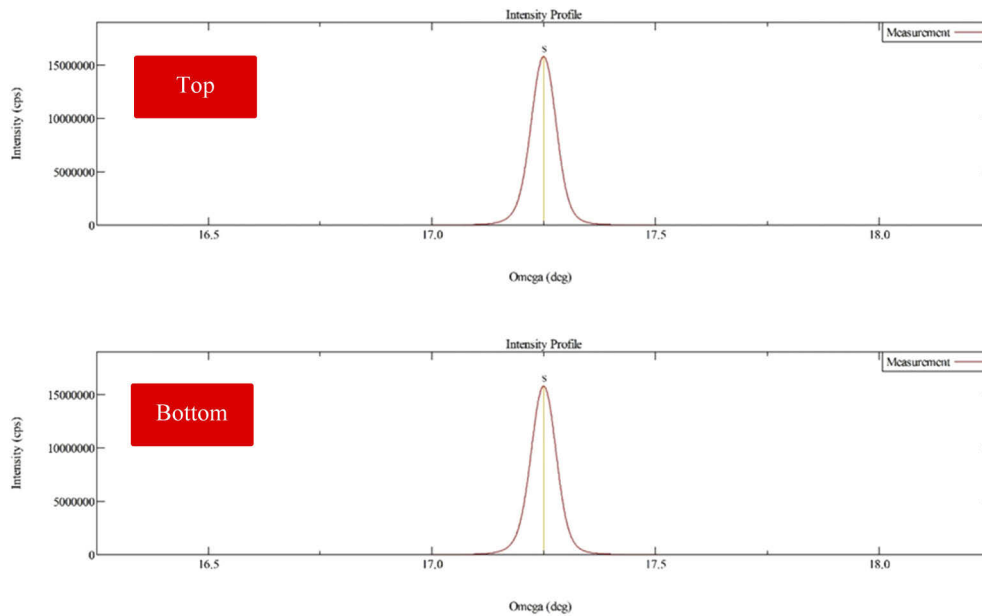


**Fig. 4.** The omega2theta result for sample B before annealing (top) and after annealing (bottom).

thickness that is bulkier, which is in micron order. We can deduce the existence of high-quality single-crystalline within the sample. For samples C and E, in which we flowed extra $NH_3$ to improve the crystal quality, the same value was obtained. This situation occurred due to the use of GaN substrate that reduces the lattice mismatch. Other samples also exhibit the same quality before and after the annealing process.

### 3.3.  TEM cross-section image

Figure 5 shows the cross-section Transmission Electron Microscopy (TEM) image of the samples. Figure 5(a) represents the cross-section of Sample A after the annealing process, while Fig. 5(b) shows the TEM image for Sample B before the annealing process, and Fig. 5(c) is the TEM image for sample B after the annealing process. Using these images, the structural condition of the MQW prior to and post the annealing process to activate the p-type can be observed and compared. The images show good contrast in the MQW's, showing the abruptness of the MQW layer of the device. The image of $In_xGa_{1-x}N$ /GaN showshomogenous layers. The total thickness of the MQW's was ~105 nm, with the $In_xGa_{1-x}N$ layers average around 3-4 nm and GaN barriers in between them were ~17 nm. These thickness are almost the same as the designed structure within the error of 25-50%. The thickness obtained here is also consistent with the XRD measurement in section 3.2. Figure 5(a) shows a darker region in contrast beneath the MQW, which can be seen as the indium that out diffused from the MQW, thus shifting the LED wavelength towards the blue region. In Fig. 5(b), we can observe the slightly darker contrast beneath the MQW in the *n*-type region. This is the Indium-riched crystal layer that formed from the TMI pre-flow. Although this layer reduces the abruptness of the barrier at the interface between the *n*-type and the MQW, the homogenous layer of the $In_xGa_{1-x}N$ layer can still be observed. In Fig. 5(c) the darker region had reduced, which can be observed as the depletion of the indium through diffusion during the annealing process. The indium diffuses downward into the much thicker *n*-type region, and upward into the MQW. The upward diffusion caused the green shift of the LED wavelength mentioned in the PL result in section 3.1. Even though there is a diffusion of indium into the MQW's, the abruptness of the $In_xGa_{1-x}N$/GaN pairs had not been affected. Contrary, the image proved that the structure of sample B after annealing keeps
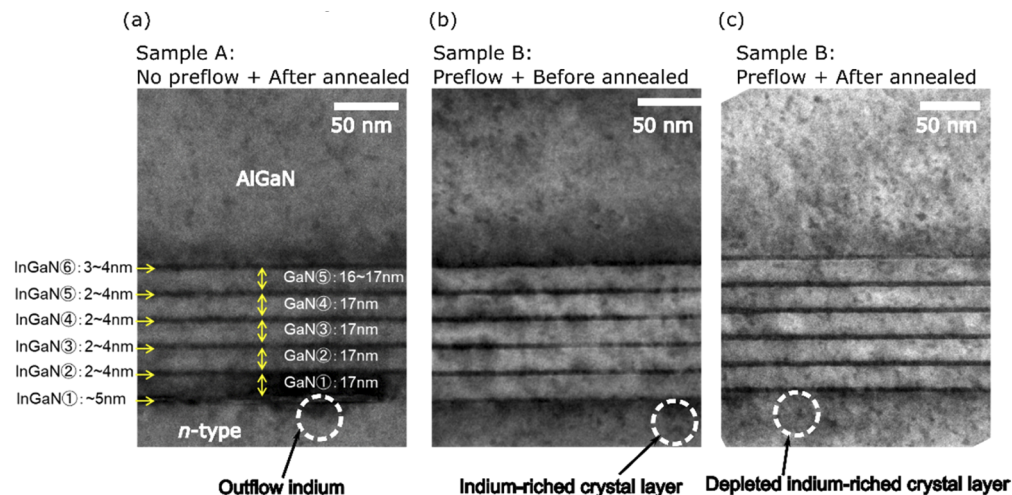


**Fig. 5.** Cross-section TEM image of the MQW's of a) sample A after annealed; b) sample B before annealing process and c) sample B after annealed. The thickness value in a) also applicable for b) and c).

the desired thickness compared to sample A after annealing. In summary, the TEM cross-section image of these samples shows that the indium pre-flow affect to keep the abruptness and the homogeneity of the MQW layers, and it helps improve the structure of the LED after annealing.

## 4.    Conclusions

We had conducted a full device LED epitaxy growth using MOCVD. We had grown the deep green LED, which had a relatively high MQW indium content. We proposed to reduce or prevent the blue wavelength shift due to MQW indium loss completely by applying the indium pre-flow technique. We succeeded to decrease and stop the problems. On optimum condition and recipe, we managed to shift the wavelength towards the green region, which can be concluded as the increase of indium in the MQW before activation via annealing. As far as we are concerned, we are the first one to report this finding for the deep green LED. They were some limitations in our work, such as we cannot achieve the thickness as desired for the $In_xGa_{1-x}N$ MQW layer as in our structure, which is 2 nm when the XRD and TEM result shows around 3~4 nm. The attempt to make it thinner by adjusting the source gases flow rate and the growth time resulted in no crystalized layer observed. The thickness of the $In_{(x)}Ga_{(1-x)}N$ creates a trade-off between the intensity of the emitted light from the indium content and the indium outflow from the MQW itself. The Indium pre-flow, as a form of treatment, proved to prevent the blue-shift, gained green shift, and improved the abruptness of the MQW layers after annealing. These findings might help in future works, especially regarding research involving MQW with high indium content, not just green but yellow and red wavelength range. The crystal quality of the samples also shows good results for a crystal in general and LED specifically.

**Disclosures.** The authors declare no conflicts of interest.

## References

1. H. Wu, X. Zhang, C. Guo, J. Xu, M. Wu, and Q. Su, "Three-band white light from InGaN-based blue LED chip precoated with Green/red phosphors," IEEE Photonics Technol. Lett. **17**(6), 1160–1162 (2005).
2. K. P. O'Donnell, I. Fernandez-Torrente, P. R. Edwards, and R. W. Martin, "The composition dependence of the InxGa$_{1-x}$N bandgap," J. Cryst. Growth **269**(1), 100–105 (2004).
3. A. Mills, "Solid state lighting — a world of expanding opportunities at LED 2002," Iii-vs Rev **16**(1), 30–33 (2003).
4. L. Peretto, E. Pivello, R. Tinarelli, and A. E. Emanuel, "Theoretical analysis of the physiologic mechanism of luminous variation in eye-brain system," IEEE Trans. Instrum. Meas. **56**(1), 164–170 (2007).
5. Y. Aoyagi, *Optical Properties of Advanced Materials*, Springer Series in Materials Science (Springer, 2013).
6. H. Haas, L. Yin, Y. Wang, and C. Chen, "What is LiFi?" J. Lightwave Technol. **34**(6), 1533–1544 (2016).
7. S. A. A. Rais, H. Najihah, Z. Hassan, and A. Shuhaimi, "Fabrication of InxGa$_{1-x}$N/GaN multi-quantum well structure for green light emitting diode on patterned sapphire substrate by metal organic chemical vapour deposition," Solid State Phenom. **290**, 147–152 (2019).
8. R. E. Eckert and H. G. Drickamer, "Diffusion in indium near the melting point," J. Chem. Phys. **20**(1), 13–17 (1952).
9. J. J. Métois and J. C. Heyraud, "SEM studies of equilibrium forms: Roughening transition and surface melting of indium and lead crystals," Ultramicroscopy **31**(1), 73–79 (1989).
10. M. U. Pralle, N. Moelders, M. P. McNeal, I. Puscasu, A. C. Greenwald, J. T. Daly, E. A. Johnson, T. George, D. S. Choi, I. El-Kady, and R. Biswas, "Photonic crystal enhanced narrow-band infrared emitters," Appl. Phys. Lett. **81**(25), 4685–4687 (2002).
11. S. Nakamura, T. Mukai, M. Senoh, and N. Iwasa, "Thermal annealing effects on P-type Mg-doped GaN films," Jpn. J. Appl. Phys. **31**(Part 2, No. 2B), L139–L142 (1992).
12. H. W. Jang and J.-L. Lee, "Effect of Cl$_2$ plasma treatment on metal contacts to n-type and p-type GaN," J. Electrochem. Soc. **150**(9), G513 (2003).

13. S. A. b. A. Rais, Z. Hassan, A. S. b. A. Bakar, M. N. b. A. Rahman, Y. b. Yusuf, M. I. b. M. Taib, A. F. b. Sulaiman, H. N. b. Hussin, and M. F. b. Ahmad, "Fabrication of deep green light emitting diode on bulk gallium nitride substrate," J. Phys.: Conf. Ser. **1535**(1), 012016 (2020).

14. T. Mukai, M. Yamada, and S. Nakamura, "Characteristics of InGaN-based UV/blue/green/amber/red light-emitting diodes," Jpn. J. Appl. Phys. **38**(7R), 3976 (2014).

15. S. Nakamura, T. Mukai, and M. Senoh, "High-brightness InGaN/AlGaN double-heterostructure blue-green-light-emitting diodes," J. Appl. Phys. **76**(12), 8189–8191 (1994).

16. M.-S. Oh, M.-K. Kwon, I.-K. Park, S.-H. Baek, S.-J. Park, S. H. Lee, and J. J. Jung, "Improvement of green LED by growing p-GaN on In0.25GaN/GaN MQWs at low temperature," J. Cryst. Growth **289**(1), 107–112 (2006).

17. W. Lee, J. Limb, J.-H. Ryou, D. Yoo, T. Chung, and R. D. Dupuis, "Effect of thermal annealing induced by p-type layer growth on blue and green LED performance," J. Cryst. Growth **287**(2), 577–581 (2006).

18. S. Nakamura, "Growth of InxGa$_{1-x}$N compound semiconductors and high-power InGaN/AlGaN double heterostructure violet-light-emitting diodes," Microelectron. J. **25**(8), 651–659 (1994).

19. S. Guha, J. M. DePuydt, M. A. Haase, J. Qiu, and H. Cheng, "Degradation of II-VI based blue-green light emitters," Appl. Phys. Lett. **63**(23), 3107–3109 (1993).

20. S. Nakamura, "The roles of structural imperfections in InGaN-based blue light-emitting diodes and laser diodes," Science **281**(5379), 956–961 (1998).

21. O. Reentilä, F. Brunner, A. Knauer, A. Mogilatenko, W. Neumann, H. Protzmann, M. Heuken, M. Kneissl, M. Weyers, and G. Tränkle, "Effect of the AlN nucleation layer growth on AlN material quality," J. Cryst. Growth **310**(23), 4932–4934 (2008).

22. Z. Deng, Y. Jiang, Z. Ma, W. Wang, H. Jia, J. Zhou, and H. Chen, "A novel wavelength-adjusting method in InGaN-based light-emitting diodes," Sci. Rep. **3**(1), 3389 (2013).

23. Y.-J. Lee, Y.-C. Chen, and T.-C. Lu, "Improvement of quantum efficiency in green light-emitting diodes with pre-TMIn flow treatment," J. Phys. D: Appl. Phys. **44**(22), 224015 (2011).

24. M. S. Kumar, J. Y. Park, Y. S. Lee, S. J. Chung, C.-H. Hong, and E.-K. Suh, "Improved internal quantum efficiency of green emitting InGaN/GaN multiple quantum wells by in preflow for InGaN well growth," Jpn. J. Appl. Phys. **47**(2), 839–842 (2008).

25. Y. Shirakawa and H. Kukimoto, "Near-band-edge photoluminescence in ZnSe grown from indium solution," J. Appl. Phys. **51**(4), 2014 (1980).

26. M. Pophristic, F. H. Long, C. A. Tran, and I. T. Ferguson, "Time-resolved photoluminescence measurements of InGaN light-emitting diodes," Mater. Sci. Forum **338-342**, 1623–1626 (2000).

27. A. V. Lobanova, K. M. Mazaev, R. A. Talalaev, M. Leys, S. Boeykens, K. Cheng, and S. Degroote, "Effect of V/III ratio in AlN and AlGaN MOVPE," J. Cryst. Growth **287**(2), 601–604 (2006).

28. S. A. Dayeh, E. T. Yu, and D. Wang, "III−V nanowire growth mechanism: V/III ratio and temperature effects," Nano Lett. **7**(8), 2486–2490 (2007).

29. G. Orsal, Y. E. Gmili, N. Fressengeas, J. Streque, R. Djerboub, T. Moudakir, S. Sundaram, A. Ougazzaden, and J. P. Salvestrini, "Bandgap energy bowing parameter of strained and relaxed InGaN layers," Opt. Mater. Express **4**(5), 1030 (2014).

30. B. Heying, X. H. Wu, S. Keller, Y. Li, D. Kapolnek, B. P. Keller, S. P. DenBaars, and J. S. Speck, "Role of threading dislocation structure on the x-ray diffraction peak widths in epitaxial GaN films," Appl. Phys. Lett. **68**(5), 643–645 (1996).

31. K. Kobayashi, A. A. Yamaguchi, S. Kimura, H. Sunakawa, A. Kimura, and A. Usui, "X-Ray rocking curve determination of twist and tilt angles in GaN films grown by an epitaxial-lateral-overgrowth technique," Jpn. J. Appl. Phys. **38**(Part 2, No. 6A/B), L611–L613 (1999).

32. J. C. Zhang, D. G. Zhao, J. F. Wang, Y. T. Wang, J. Chen, J. P. Liu, and H. Yang, "The influence of AlN buffer layer thickness on the properties of GaN epilayer," J. Cryst. Growth **268**(1-2), 24–29 (2004).